UtilitasMathematica

ISSN 0315-3681 Volume 122, 2025

Effect of Soret on Unsteady MHD Casson Fluid Flow over a Vertical Surface using Laplace Transformation

S. Dinesh[1] S. Lakshmi Priya[2] *

[1]Department of Mathematics and Statistics,
Faculty of Science and Humanities,
SRM Institute of Science and Technology,
Kattankulathur 603203, Chengalpattu, INDIA
Mail: ds7870@srmist.edu.in

[2]Department of Mathematics and Statistics,
Faculty of Science and Humanities,
SRM Institute of Science and Technology,
Kattankulathur 603203, Chengalpattu, INDIA
Mail: lakshmis3@srmist.edu.in

ABSTRACT: The unsteady magnetohydrodynamic (MHD) flow of a Casson fluid along an infinite vertical surface that is exponentially stretching is studied analytically in this paper, taking into account the Soret effect. By taking into account the Soret effect, the study expands on current approaches that use the Laplace transform to unravel the flow model's governing equations. A series of coupled partial derivative equations addressing the momentum, energy, and concentration distributions characterize the system's behaviour. The model incorporates a chemical reaction parameter, magnetic field effects, and Casson fluid properties into the equations. The Laplace transform technique is adopted to derive a solution. The study emphasizes how velocity, temperature, and concentration profiles are altered by changes in the chemical reaction parameter. Furthermore, the consequence of variables like magnetic field strength M, Casson fluid parameter β, Grashof number Gr, Prandtl number Pr, thermal radiation Rd, Schmidt number Sc, and Prandtl number Pr are all carefully investigated. The results contribute to a better understanding of MHD flows in Casson fluids and their significance in heat and mass transfer systems by providing insightful information for improving industrial processes involving the interaction of magnetic fields and non-Newtonian fluids under the dominance of the Soret effect.

KEYWORDS: MHD, Soret effect, Chemical reaction, Thermal radiation, Casson fluid

INTRODUCTION:

Examining the Soret effect in unstable MHD The practical significance of Casson fluid flow in astrophysics, geophysics, energy reactors, power generation, petroleum

engineering, and boundary layer control—including cooling systems in reactors has drawn attention. Casson fluids, which are known to show yield stress, have been studied by numerous researchers. Casson fluids are non-Newtonian and have a variable viscosity that varies with the applied stress, in contrast to Newtonian fluids. In many industrial settings, it is essential to comprehend their rheological behaviour. These real-world uses have led to a number of studies investigating Casson fluid flow models. The physical behaviour of Casson fluids is being investigated more thoroughly because of its many applications. The preliminary goal of this inquiry is to analyse the mass transmission and heat properties of an unsteady MHD flow of a Casson fluid alongside an unbounded upright surface that is exponentially stretching. The fluid is exposed to an externally exerted magnetic field and is chemically reactive. This work is inspired by several previous studies. An logical solution for MHD convective flow along a permeable medium was presented by [1]Pattnaik.P.K and Biswal.T., taking into account temperature and concentration variations over time. They concentrated on analytically resolving the governing equations for momentum, energy, and concentration. An unsteady MHD advection flow of Casson fluid over an upright undulating plate situated within a permeable medium was probed by [2] Khalid. A, Shafie.S, and Khan.A in a different study. [3]Mukhopadhyay.S investigated the role of thermal radiation in a Casson fluid flow over an unstable tensile surface with surface extraction. Later, in 2014, [4]Pramanik.S examined the heat transfer in Casson fluid across an exponentially porous extending surface, paying particular attention to the aftermath of thermal radiation on the temperature profile. In [5], Arthur, E.M., Seini, I.Y., and Bortteir, L.B. investigated the Casson fluid across an upright permeable surface while a chemical reaction and an external magnetic field were present. Under these circumstances, they were able to pinpoint the precise flow characteristics. Heat and mass transmission in a counteracting chemical and heat-engulfing fluid alongside an engulfing plate were investigated in 2017 [6] by Seth.G.S et al.They worked on the built up wall temperature and hydromagnetic spontaneous convection, and they came up with an exact analytical solution. By incorporating Hall current effects, this study was expanded even further. Subsequently, [7]Mahato.G.K et al. examined the effects of rotation and Hall currents on hydro magnetic passive advection while taking heat sources, chemical reactions, and external magnetic fields into account. [8] Talha Anwar, Poomkumam, and Wiboonsak Watthayu conducted a thorough investigation of unsteady MHD Casson fluid with radiating emission and injection/suction at the boundary. Their research took into account different wall conditions and shed light on how these boundaries affect Casson fluid behaviour. In 2016, [9]Ojjela.O et al. investigated the transient MHD hibrid convective flow of a thermally radiative, chemically reactive torque stress fluid in a permeable channel amid coaxial plates while taking Dufour effects into account. [10] Unforced convective heat and mass transfer in Casson fluids in unstable, transmissive extending surfaces, including viscous attenuation, were thoroughly examined by Shateyi.S, Mahmood.F, and Lorenzini.G. More recently, [11]Hanumesh.V et al. investigated the joint implications of changing thermal conductivity and chemical reaction in an MHD contractile flow of a Phan-Thien-Tanner fluid through an oblique channel. [12] Anwar et al. examined MHD fluid flow along an

expanding sheet in a computational study. Additionally, nonlinear MHD flow between parallel walls under the persuasion of surface roughness was inquired by [13] Abbas et al. and [14] Ammar et al., highlighting modifications in flow behaviour brought on by external constraints.

Unsteady MHD flows involving non-Newtonian and Casson fluids were examined by Farhan Ali et al. in 2023 [15] using variables such as internal heat generation, thermal radiation, and variable Prandtl and Schmidt numbers. The flow was started in their study by applying external magnetic fields. Building on these studies, the current investigation incorporates into the governing equations the effects of chemical reactions as well as the Soret effect, in which a concentration gradient affects the temperature field. The growing significance of these interactions in real-world applications is reflected in this extension. A thorough examination of fluid motion across an infinite vertical surface that stretches exponentially is provided, in which a magnetic field is employed to the system. The governing equations and boundary constraints are transmuted into a Non-dimensional form through non-dimensional variables. The momentum, energy, and concentration fields are analytically sorted out using Laplace transform techniques. MATLAB is used to graphically present the results so that the flow behaviour can be readily comprehended.

MATHEMATICAL FORMULATION:

Let us investigate the MHD Casson fluid with existence of the consequence of Soret, thermal radiation, heat source and the chemically reactive fluid flow through a vertical surface. Initially when the demonstration takes place, the velocity profile is taken under consideration. Additionally, the magnetic strength of the field is accounted in the opposite x-axis. Further, when t = 0, the velocity is U = e^{at} for all the above stated conditions, the initial governing equations are derived from the Boussinesq's approximation. Where u signifies velocity coordinate in x-axis and v signifies velocity coordinate in y-axis. The flow is in accordance with the kinematic viscosity is denoted as ν, T is the Temperature of fluid and T_∞ is the ambient temperature and the concentration field is C and C_∞ is the ambient concentration. ρ denotes the fluid density, t is the time, the magnetic field is denoted as B_0 and electrical conductivity is σ.

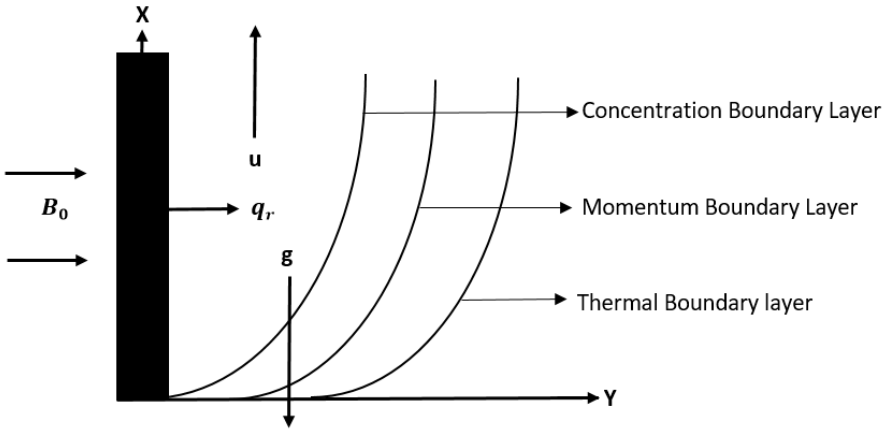

Figure : 1

Therefore the respective governing equations are as follows

Momentum equation:

$$\frac{\partial u}{\partial t'} = g\beta'(T - T_\infty) + g\beta^*(C - C_\infty) + v\left(1 + \frac{1}{\beta}\right)\frac{\partial^2 u}{\partial y^2} - \frac{\sigma B_0^2}{\rho}u \tag{1}$$

Energy equation:

$$\rho C_p \frac{\partial T}{\partial t'} = k\frac{\partial^2 T}{\partial y^2} - Q_0(T - T_\infty) - \frac{\partial q_r}{\partial y} \tag{2}$$

Concentration equation:

$$\frac{\partial C}{\partial t'} = D\frac{\partial^2 C}{\partial y^2} - Kr\,(C - C_\infty) + \frac{D_m V K_m}{C_s}\frac{\partial^2 T}{\partial y^2} \tag{3}$$

Boundary conditions:

$$\left.\begin{array}{llll} u = 0, & T = T_\infty, & C = C_\infty & \text{for all } y \text{ and } t' \geq 0 \\ u = u_0, & T = T_W, & C = C_W & \text{at } y = 0 \\ u = 0, & T = T_W, & C = C_W & \text{at } y \to 0 \end{array}\right\} \tag{4}$$

Local gradient:

$$\frac{\partial q_r}{\partial y} = -4b^*\sigma\,(T_\infty^4 - T^4) \tag{5}$$

By implying Taylor's theorem and eliminating higher derivatives, we get

$$T^4 \cong 4T_\infty^3 T - 3T_\infty^4 \quad (6)$$

By utilizing (5) and (6) in (2), it becomes

$$\rho C_p \frac{\partial T}{\partial t'} = K\frac{\partial^2 T}{\partial y^2} - Q_0(T - T_\infty) - 16b^*\sigma T_\infty^3(T - T_\infty) \quad (7)$$

Non-Dimensional variables are as follows:

$U = \frac{u}{u_0}$; $t = \frac{t'u_0^2}{v}$; $Y = \frac{yu_0}{v}$; $S_c = \frac{v}{D}$;

$\theta = \frac{T - T_\infty}{T_w - T_\infty}$; $\varphi = \frac{C - C_\infty}{C_w - C_\infty}$; $Gr = \frac{gv\beta'(T_w - T_\infty)}{u_0^3}$; $Gc = \frac{gv\beta^*(C_w - C_\infty)}{u_0^3}$;

$Kr = \frac{Ku_0^2}{v}$; $Rd = \frac{16\sigma b^* v^2 T_\infty^3}{ku_0^2}$; $Pr = \frac{\rho v C_p}{k}$; $Sr = \frac{D_m\ K_m}{C_s}\frac{T_w - T_\infty}{C_w - C_\infty}$

Implementing the Non-Dimensional quantities in (1), (3) and (7)

$$\frac{\partial U}{\partial t} = \left(1 + \frac{1}{\beta}\right)\frac{\partial^2 U}{\partial Y^2} + Gr\theta + Gc\varphi - MU \quad (8)$$

$$\frac{\partial \theta}{\partial t} = \frac{1}{P_r}\frac{\partial^2 \theta}{\partial Y^2} - Q\theta - Rd\theta \quad (9)$$

$$\frac{\partial \varphi}{\partial t} = \frac{1}{S_c}\frac{\partial^2 \varphi}{\partial Y^2} - K\varphi + Sr\frac{\partial^2 \theta}{\partial Y^2} \quad (10)$$

The boundary conditions:

$U = 0;$	$\theta = 0;$	$\varphi = 0;$	$for\ all\ Y\ and\ t \leq 0$
$U = e^{at};$	$\theta = 1;$	$\varphi = 1;$	$at\ Y = 0$
$U \to 0;$	$\theta \to 0;$	$\varphi \to 0;$	$at\ Y \to \infty$

We can now acquire the outcome of the flow model by incorporating the technique of Laplace Transformation with respect to time in the equations (8), (9) and (10). Hence the resultant Laplace equations are as follows:

$$L(U) = \frac{e^{-y\sqrt{\frac{s+M}{\beta_0}}}}{s} - Gr\frac{R_1}{R_2}\left[\frac{e^{-y\sqrt{Pr\,(s+\alpha)}}}{s}\right] + Gr\frac{R_1}{R_2}\left[\frac{e^{-y\sqrt{Pr\,(s+\alpha)}}}{s+R_2}\right] - Gc\frac{R_3}{R_4}\left[\frac{e^{-y\sqrt{Sc\,(s+K)}}}{s}\right] + Gc\frac{R_3}{R_4}\left[\frac{e^{-y\sqrt{Sc\,(s+K)}}}{s+R_4}\right] - Gc\frac{R_1}{R_2}Sr(Pr.\alpha + Pr.s)\left[\frac{e^{-y\sqrt{Pr\,(s+\alpha)}}}{s}\right] + Gc\frac{R_1}{R_2}Sr(Pr.\alpha + Pr.s)\left[\frac{e^{-y\sqrt{Pr\,(s+\alpha)}}}{s+R_2}\right] - Gc\frac{R_3}{R_4}Sr(Sc.k + Sc.s)\left[\frac{e^{-y\sqrt{Sc\,(s+K)}}}{s}\right] + Gc\frac{R_3}{R_4}Sr(Sc.k + Sc.s)\left[\frac{e^{-y\sqrt{Sc\,(s+K)}}}{s+R_4}\right] \quad (11)$$

$$L(\theta) = \left[\frac{e^{-y\sqrt{Pr\,(s+\alpha)}}}{s}\right] \quad (12)$$

$$L(\varphi) = \left[\frac{e^{-y\sqrt{Sc\,(s+K)}}}{s}\right] + Sr\,\frac{q_1}{q_2}\left[\frac{e^{-y\sqrt{Pr\,(s+\alpha)}}}{s}\right] - Sr\,\frac{q_1}{q_2}\left[\frac{e^{-y\sqrt{Pr\,(s+\alpha)}}}{s+q_2}\right] + Sr\,\frac{q_3}{q_4}\left[\frac{e^{-y\sqrt{Sc\,(s+K)}}}{s}\right] - Sr\,\frac{q_3}{q_4}\left[\frac{e^{-y\sqrt{Sc\,(s+K)}}}{s+q_4}\right] \quad (13)$$

Following these Laplace equations, the final solutions of the equations (11), (12) and (13) are attained by incorporating the Inverse Laplace transforms. The resulting solutions are as follows:

$$\varphi = \frac{e^{kt}}{2}\left[e^{-y\sqrt{Sc.k}}\,erfc\left(\eta\sqrt{Sc} - \sqrt{kt}\right) + e^{y\sqrt{Sc.k}}\,erfc\left(\eta\sqrt{Sc} + \sqrt{kt}\right)\right] + Sr\,\frac{q_1}{q_2}\,\frac{e^{\alpha t}}{2}\left[e^{-y\sqrt{Pr.\alpha}}\,erfc\left(\eta\sqrt{Pr} - \sqrt{\alpha t}\right) + e^{y\sqrt{Pr.\alpha}}\,erfc\left(\eta\sqrt{Pr} + \sqrt{\alpha t}\right)\right] - Sr\frac{q_1}{q_2}\frac{e^{(\alpha-q_2)t}}{2}\left[e^{-y\sqrt{Pr(\alpha-q_2)}}\,erfc\left(\eta\sqrt{Pr} - \sqrt{(\alpha-q_2)t}\right) + e^{y\sqrt{Pr(\alpha-q_2)}}\,erfc\left(\eta\sqrt{Pr} + \sqrt{(\alpha-q_2)t}\right)\right] + Sr\,\frac{q_3}{q_4}\,\frac{e^{kt}}{2}\left[e^{-y\sqrt{Sc.k}}\,erfc\left(\eta\sqrt{Sc} - \sqrt{kt}\right) + e^{y\sqrt{Sc.k}}\,erfc\left(\eta\sqrt{Sc} + \sqrt{kt}\right)\right] - Sr\,\frac{q_3}{q_4}\,\frac{e^{(k-q_4)t}}{2}\left[e^{-y\sqrt{Sc(k-q_4)}}\,erfc\left(\eta\sqrt{Sc} - \sqrt{(k-q_4)t}\right) + e^{y\sqrt{Sc(k-q_4)}}\,erfc\left(\eta\sqrt{Sc} + \sqrt{(k-q_4)t}\right)\right] \quad (14)$$

$$\theta = \frac{e^{\alpha t}}{2}\left[e^{-y\sqrt{Pr.\alpha}}\,erfc\left(\eta\sqrt{Pr} - \sqrt{\alpha t}\right) + e^{y\sqrt{Pr.\alpha}}\,erfc\left(\eta\sqrt{Pr} + \sqrt{\alpha t}\right)\right] \quad (15)$$

$$U = \frac{e^{Mt}}{2}\left[e^{-y\sqrt{\frac{M}{\beta_0}}}\, erfc\left(\frac{\eta}{\sqrt{\beta_0}} - \sqrt{Mt}\right) + e^{y\sqrt{\frac{M}{\beta_0}}}\, erfc\left(\frac{\eta}{\sqrt{\beta_0}} + \sqrt{Mt}\right)\right]$$

$$-\mathrm{Gr}\frac{\mathrm{R}_1}{\mathrm{R}_2}\frac{e^{\alpha t}}{2}\left[e^{-y\sqrt{Pr.\alpha}}\, erfc\left(\eta\sqrt{Pr} - \sqrt{\alpha t}\right) + e^{y\sqrt{Pr.\alpha}}\, erfc\left(\eta\sqrt{Pr} + \sqrt{\alpha t}\right)\right]$$

$$+\mathrm{Gr}\frac{\mathrm{R}_1}{\mathrm{R}_2}\frac{e^{(\alpha-\mathrm{R}_2)t}}{2}\left[e^{-y\sqrt{\mathrm{Pr}(\alpha-\mathrm{R}_2)}}\, erfc\left(\eta\sqrt{Pr} - \sqrt{(\alpha-\mathrm{R}_2)t}\right) + e^{y\sqrt{\mathrm{Pr}(\alpha-\mathrm{R}_2)}}\, erfc\left(\eta\sqrt{Pr} + \sqrt{(\alpha-\mathrm{R}_2)t}\right)\right]$$

$$-\mathrm{Gc}\frac{\mathrm{R}_3}{\mathrm{R}_4}\frac{e^{kt}}{2}\left[e^{-y\sqrt{Sc.k}}\, erfc\left(\eta\sqrt{Sc} - \sqrt{kt}\right) + e^{y\sqrt{Sc.k}}\, erfc\left(\eta\sqrt{Sc} + \sqrt{kt}\right)\right]$$

$$+\mathrm{Gc}\frac{\mathrm{R}_3}{\mathrm{R}_4}\frac{e^{(k-\mathrm{R}_4)t}}{2}\left[e^{-y\sqrt{Sc(k-\mathrm{R}_4)}}\, erfc\left(\eta\sqrt{Sc} - \sqrt{(k-R_4)t}\right) + e^{y\sqrt{Sc(k-\mathrm{R}_4)}}\, erfc\left(\eta\sqrt{Sc} + \sqrt{(k-\mathrm{R}_4)t}\right)\right]$$

$$-\mathrm{Gc}\frac{\mathrm{R}_1}{\mathrm{R}_2}Sr(\mathrm{Pr}.\alpha + \mathrm{Pr}.\mathrm{s})\frac{e^{\alpha t}}{2}\left[e^{-y\sqrt{Pr.\alpha}}\, erfc\left(\eta\sqrt{Pr} - \sqrt{\alpha t}\right) + e^{y\sqrt{Pr.\alpha}}\, erfc\left(\eta\sqrt{Pr} + \sqrt{\alpha t}\right)\right]$$

$$+\mathrm{Gc}\frac{\mathrm{R}_1}{\mathrm{R}_2}Sr(\mathrm{Pr}.\alpha + \mathrm{Pr}.\mathrm{s})\frac{e^{(\alpha-\mathrm{R}_2)t}}{2}\left[e^{-y\sqrt{\mathrm{Pr}(\alpha-\mathrm{R}_2)}}\, erfc\left(\eta\sqrt{Pr} - \sqrt{(\alpha-\mathrm{R}_2)t}\right) + e^{y\sqrt{\mathrm{Pr}(\alpha-\mathrm{R}_2)}}\, erfc\left(\eta\sqrt{Pr} + \sqrt{(\alpha-\mathrm{R}_2)t}\right)\right]$$

$$-\mathrm{Gc}\frac{\mathrm{R}_3}{\mathrm{R}_4}Sr(\mathrm{Sc}.\mathrm{k} + \mathrm{Sc}.\mathrm{s})\frac{e^{kt}}{2}\left[e^{-y\sqrt{Sc.k}}\, erfc\left(\eta\sqrt{Sc} - \sqrt{kt}\right) + e^{y\sqrt{Sc.k}}\, erfc\left(\eta\sqrt{Sc} + \sqrt{kt}\right)\right]$$

$$+\mathrm{Gc}\frac{\mathrm{R}_3}{\mathrm{R}_4}Sr(\mathrm{Sc}.\mathrm{k} + \mathrm{Sc}.\mathrm{s})\frac{e^{(k-\mathrm{R}_4)t}}{2}\left[e^{-y\sqrt{Sc(k-\mathrm{R}_4)}}\, erfc\left(\eta\sqrt{Sc} - \sqrt{(k-R_4)t}\right) + e^{y\sqrt{Sc(k-\mathrm{R}_4)}}\, erfc\left(\eta\sqrt{Sc} + \sqrt{(k-\mathrm{R}_4)t}\right)\right] \quad (16)$$

RESULTS AND DISCUSSIONS:

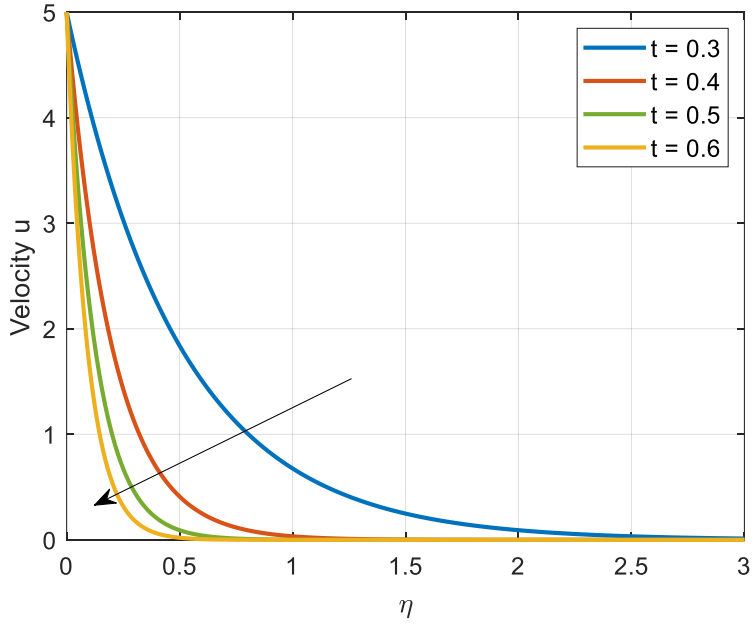

Figure 2: Effect of Velocity (u) for time (t)

Figure 2 portrays the variation of time (t = 0.3, 0.4, 0.5, 0.6) along fluid velocity. While time is increased, the thermo-momentum boundary layer also grows, which provokes an increment in the fluid velocity.

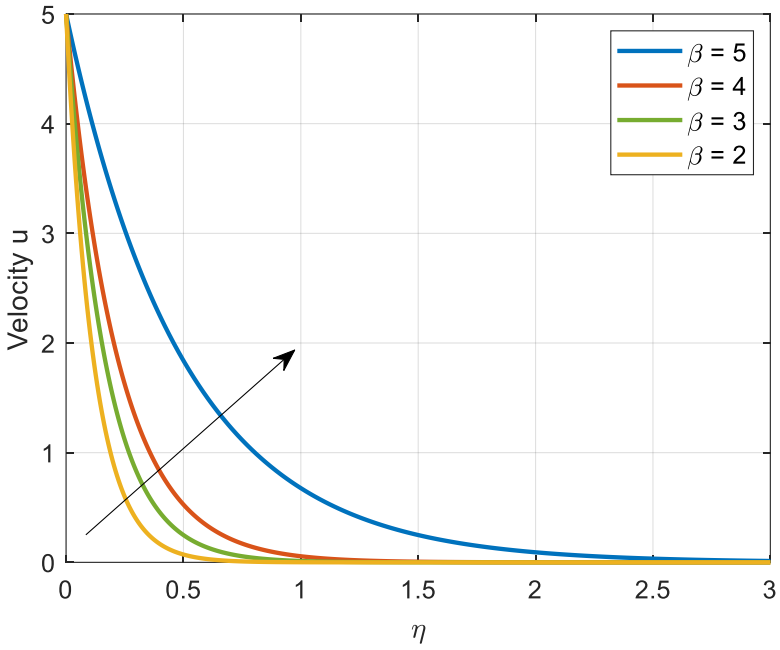

Figure 3: Effect of Velocity (u) for Casson parameter (β)

Figure 3 sketches the contribution of the Casson parameter (β = 2, 3, 4, 5) on velocity domain. The speed and viscous flow are found to decrease as the value rises. As a consequence of the Casson fluid's diminished density, its velocity is higher than that of inviscid fluids.

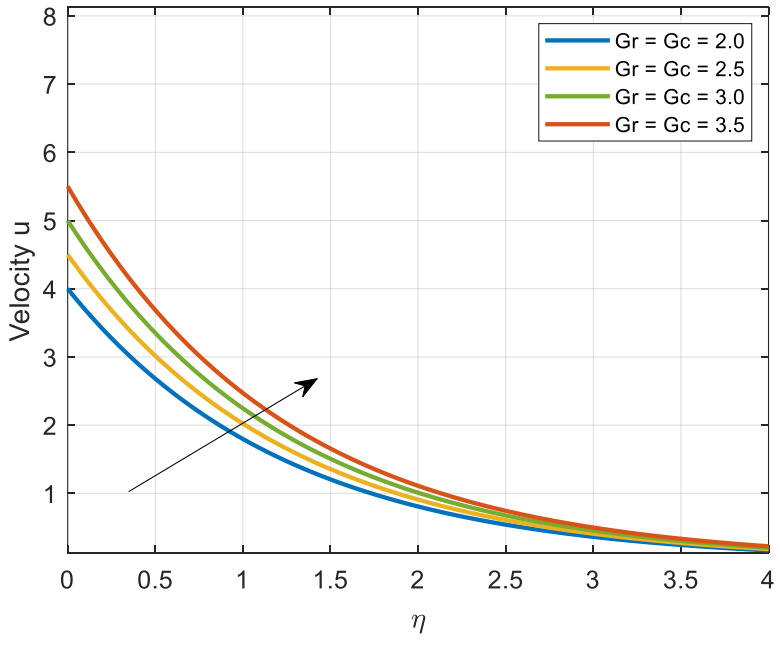

Figure 4: Effect of Velocity (u) for Grashof number

Figures 4 display the impact of Grashof number for Heat transfer (Gr = 2.0, 2.5, 3.0, 3.5) and Grashof number for Mass transfer (Gc = 2.0, 2.5, 3.0, 3.5) over fluid velocity. An upsurge in the metrics of Gr and Gc produces an enhancement of the fluid's velocity

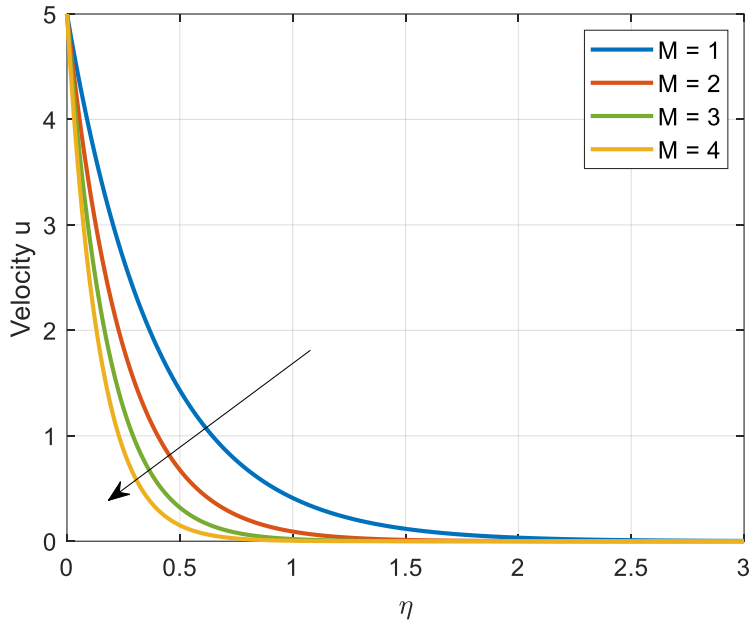

Figure 5: Effect of Velocity (u) for Magnetic parameter (M)

Figure 5 depicts the impact of the magnetic field parameter (M = 1, 2, 3, 4) on the fluid velocity. It is clear that fluid velocity falls as M elevates. Since Lorentz forces, which function as resistive forces, are yielded when a magnetic field is implied to an electrically conducting fluid, this behaviour can be physically explained. These forces typically suppress fluid motion, which lowers flow velocity and creates a thinner momentum boundary layer.

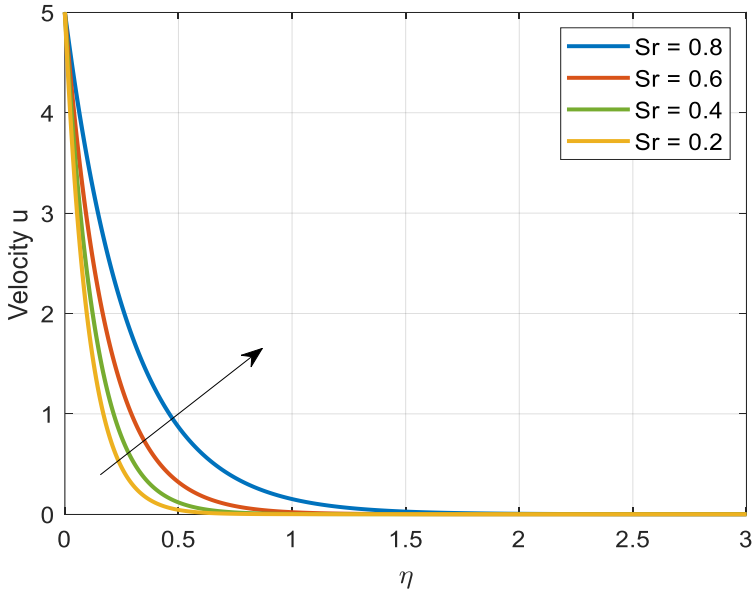

Figure 6: Effect of Velocity (u) for Soret effect (Sr)

Figure 6 shows that the increase in the Soret effect (Sr = 0.2, 0.4, 0.6, 0.8) increase the fluid velocity. This is because Buoyancy force becoming stronger due to the leverage of the Grashof number for diffusion due to the presence of Soret, culminating an elevation in the velocity of the fluid.

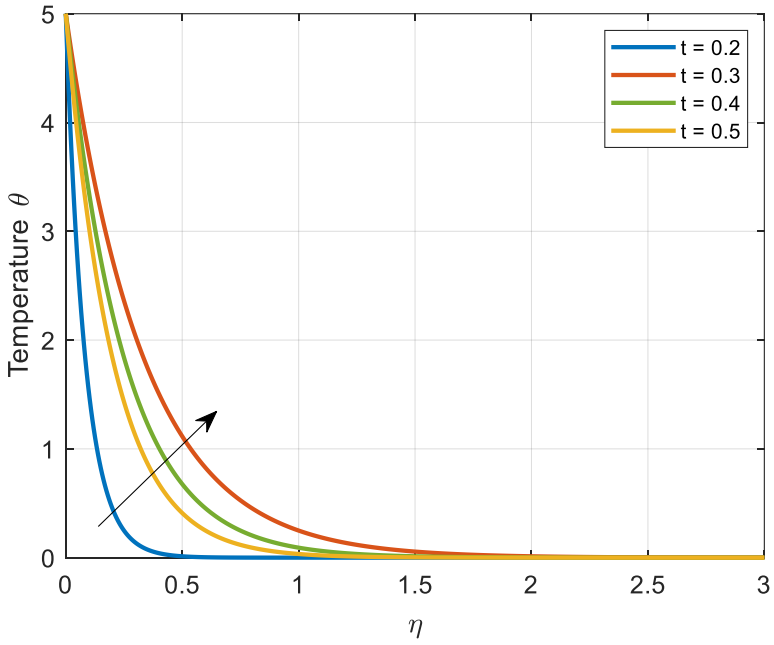

Figure 7: Effect of Temperature (θ) for time (t)

Figure 7 explains that the increase in time (t = 0.2, 0.3, 0.4, 0.5) increase the temperature of the fluid. This is the consequence of elevates in the thermo-momentum boundary layer.

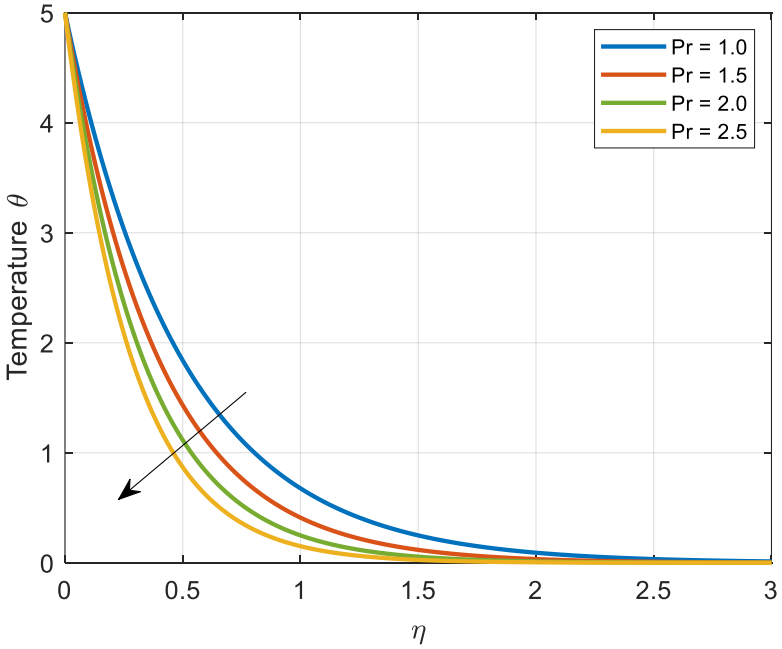

Figure 8: Effect of Temperature (θ) for Prandtl number (Pr)

Figure 8 elucidates the effects of developing the Prandtl number (Pr = 1.0, 1.5, 2.0, 2.5) on fluid temperature. Because of the greater diffusivity, the fluid temperature drops as Pr rises. This implies that thermal diffusivity is more important in the boundary layer, which causes a discernible shift in the fluid's internal temperature distribution.

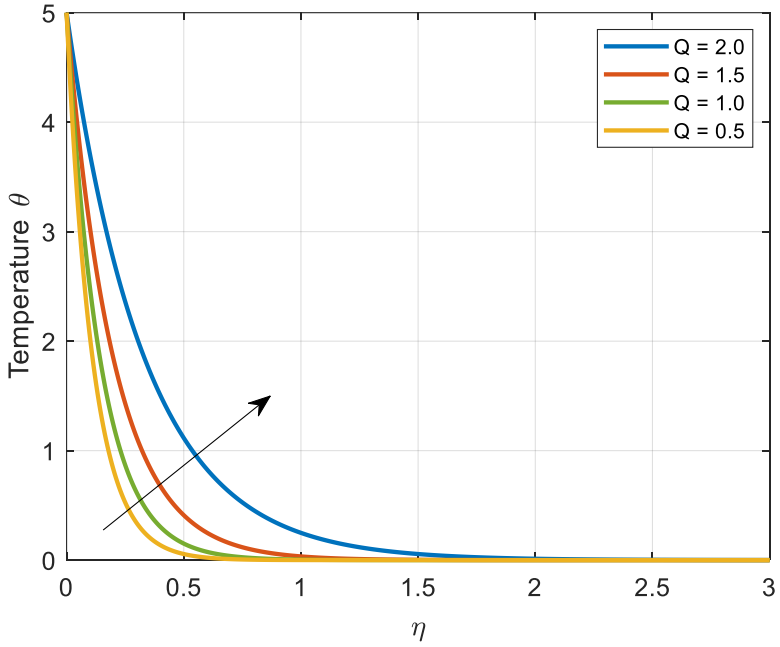

Figure 9: Effect of Temperature (θ) for Heat source (Q)

Figure 9 depicts that the temperature domain elevates with a rise in heat source (Q = 0.5, 1.0, 1.5, 2.0). Furthermore, the increase in the heat source enhances heat transfer, which in turn increases the temperature.

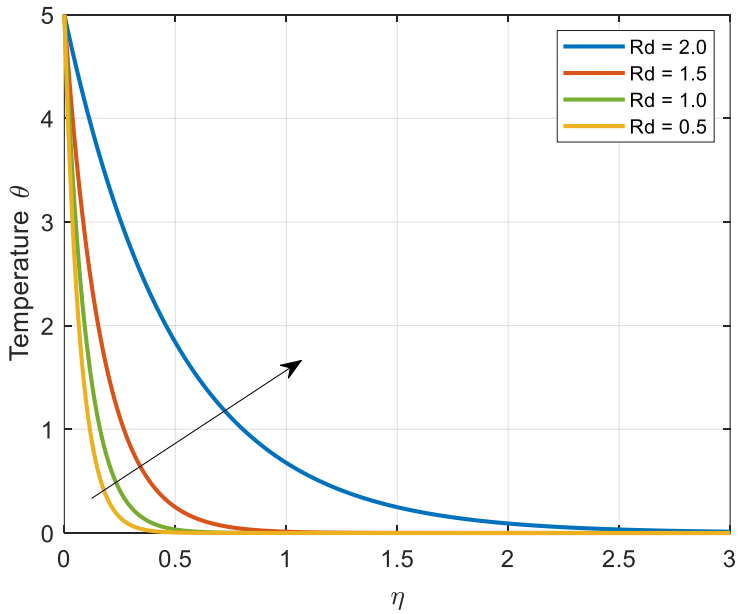

Figure 10: Effect of Temperature (θ) for Radiation parameter (Rd)

Figure 10 explains that the temperature increases as the radiation parameter (Rd = 0.5, 1.0, 1.5, 2.0) inclines. This is the consequence of enhancement of the thermal levels in the boundary layer.

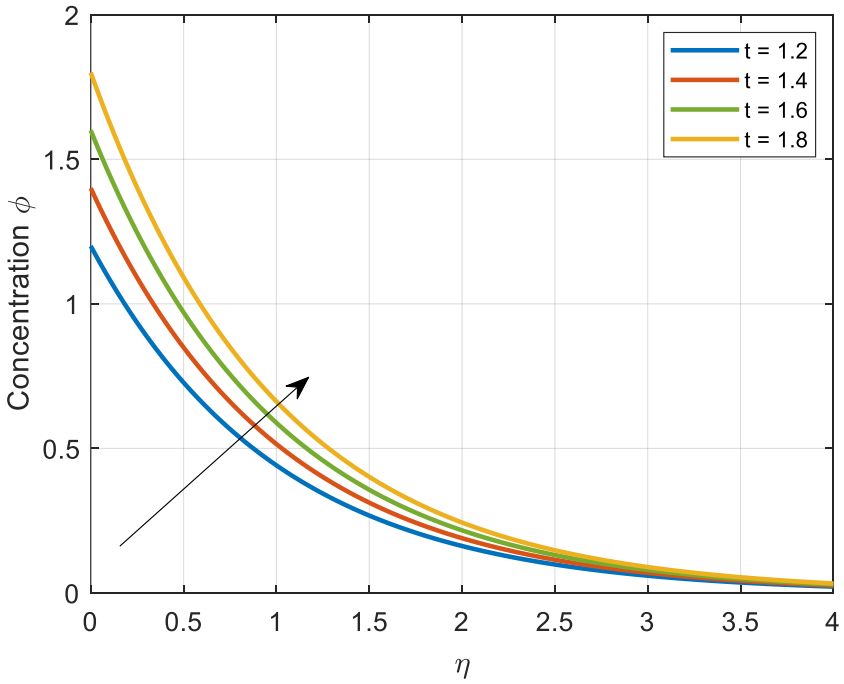

Figure 11: Effect of Concentration (φ) for time (t)

Figure 11 visualizes that the Concentration of the fluid uplifts as the time (t = 1.2, 1.4, 1.6, 1.8) increases.

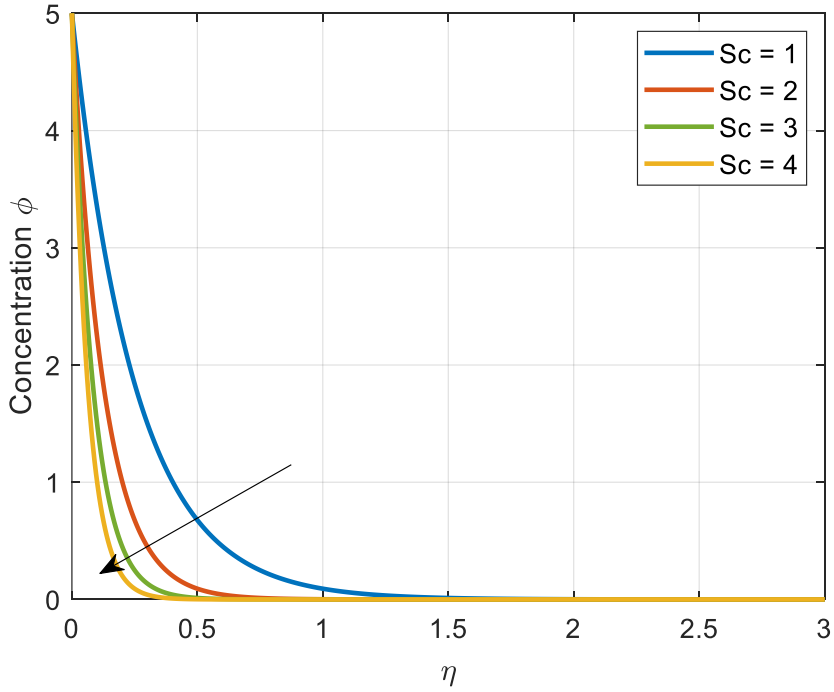

Figure 12: Effect of Concentration (φ) for Schmidt number (Sc)

Figure 12 exhibits the significance of Schmidt number (Sc = 1, 2, 3, 4) on concentration profiles. It has been found that as Schmidt numbers go up, the concentration levels and the density of the concentration boundary layer declines.

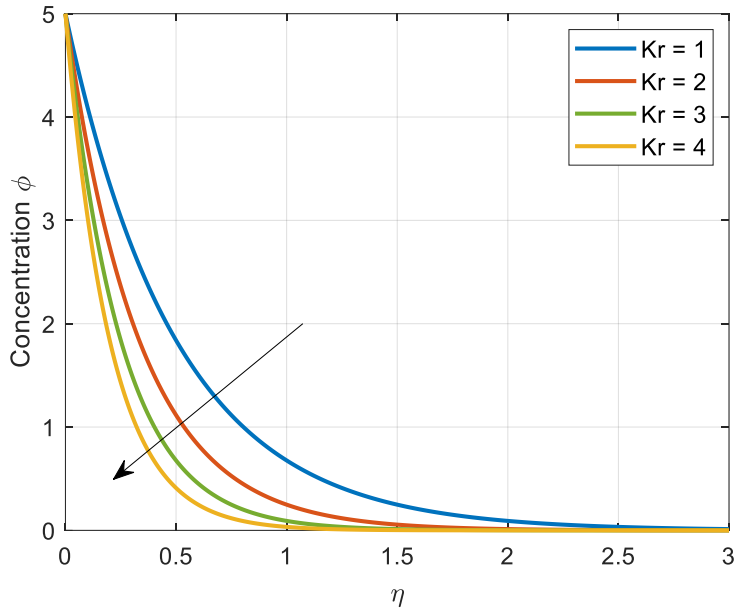

Figure 13: Effect of Concentration (φ) for Chemical reaction (Kr)

Figure 13 shows that an elevation in chemical reaction (Kr = 1, 2, 3, 4) decreases the concentration of the fluid because the reactant species are being consumed during the chemical reaction process.

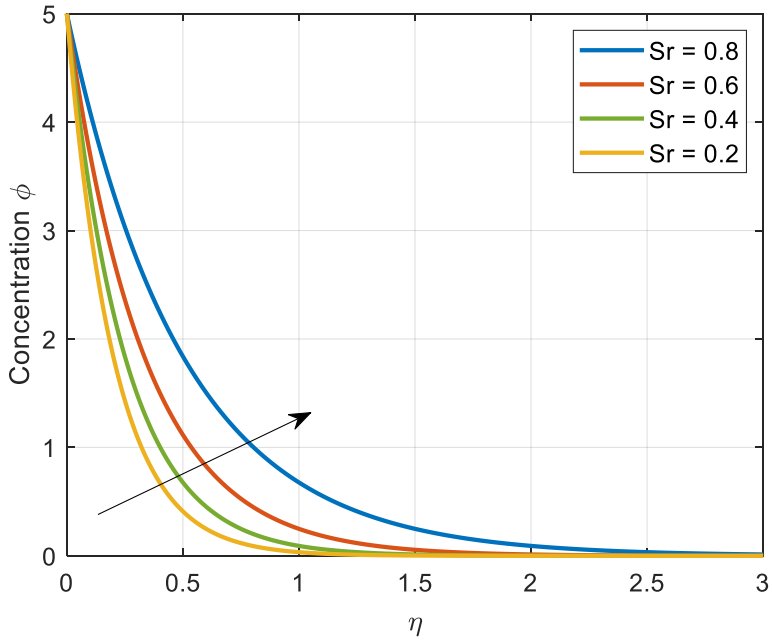

Figure 14: Effect of Concentration (φ) for Soret effect (Sr)

Figure 14 clearly shows that the increase in the Soret effect (Sr = 0.2, 0.4, 0.6, 0.8) increases the concentration of the fluid. This is because the Soret effect causes flux density due to a temperature gradient.

CONCLUSION:

This study furnishes approximate analytical solutions for a MHD casson fluid through an upright surface with occurrence of Thermal radiation, Chemical reaction and soret effect. We have arrived at the formulations for dimensionless velocity, temperature and concentration by deploying the method of Laplace transforms and portrayed graphically.

- Magnetic field reduces the fluid velocity.
- Velocity domain gains momentum due to the impact of soret effect.
- Grashof number also claims to raise the velocity of the fluid.
- Temperature enhances due to growth of thermal radiation.
- Increment in Heat source results in rapid uplifting of Temperature field.
- Temperature profile falls with a rise in Prandtl number.
- Soret effect (Sr) induces the concentration profile considerably.
- Concentration profile falls by the impact of Schmidt number.
- Enlargement in Chemical reaction leads to the decline of concentration profile.
- Graphical study justifies the study of all fields of the casson fluid.

REFERENCES:

1) Pattnaik, P. K. & Biswal, T. Analytical solution of MHD free convective flow through porous media with time dependent temperature and concentration. Walailak J. Sci. Tech. 12(9), 749–762 (2015).

2) Khalid, A., Khan, I., Khan, A. & Shafie, S. Unsteady MHD free convection flow of Casson fluid past over an oscillating vertical plate embedded in a porous medium. Eng. Sci. Technol. Int. J. 18(3), 309–317 (2015).

3) Mukhopadhyay, S. Effects of thermal radiation on Casson fluid flow and heat transfer over an unsteady stretching surface subjected to suction/blowing. Chin. Phys. B 22(11), 114702 (2013).

4) Pramanik, S. Casson fluid flow and heat transfer past an exponentially porous stretching surface in presence of thermal radiation. Ain Shams Eng. J. 5(1), 205–212 (2014).

5) Arthur, E. M., Seini, I. Y. & Bortteir, L. B. Analysis of Casson fluid flow over a vertical porous surface with chemical reaction in the presence of magnetic field. J Appl. Math. Phys. 3, 713–723 (2015).

6) Seth, G. S., Hussain, S. M. & Sarkar, S. Hydromagnetic natural convection flow with heat and mass transfer of a chemically reacting and heat absorbing fluid past an accelerated

moving vertical plate with ramped temperature and ramped surface concentration through a porous medium. J. Egyp. Math. Soc. 23(1), 197–207 (2015).

7) Seth, G. S., Sarkar, S., Hussain, S. M. & Mahato, G. K. Effects of hall current and rotation on hydromagnetic natural convection flow with heat and mass transfer of a heat absorbing fluid past an impulsively moving vertical plate with ramped temperature. J. Appl. Fluid Mech. 8(1), 159–171 (2015).

8) Talha Anwar, Poom Kumam, WiboonsakWatthayu, Unsteady MHD natural Convection flow of casson fluid incorporating thermal radiative flux and heat injection/suction mechanism under variable wall conditions. Scientifc Reports (2021) 11:4275.

9) Ojjela, O., and N. Naresh Kumar. 2016. "Unsteady MHD Mixed Convective Flow of Chemically Reacting and Radiating Couple Stress Fluid in a Porous Medium Between Parallel Plates with Soret and Dufour Effects." Arabian Journal for Science and Engineering 41: 1941–1953.

10) Shateyi, S., F. Mabood, and G. Lorenzini. 2017. "Casson Fluid Flow: Free Convective Heat and Mass Transfer Over an Unsteady Permeable Stretching Surface Considering Viscous Dissipation." Journal of Engineering Thermophysics 26 (1): 39–52.

11) V. Hanumesh, K.V. Prasad, M.I. Khan, F.M. Oudina, I. Tlili, C. Rajashekhar, *et al.* Combined effects of chemical reaction and variable thermal conductivity on MHD peristaltic flow of phan-thien-tanner liquid through inclined channel. Case Stud Therm Eng, 36 (2022).

12) M.I. Anwar, H. Firdous, A. Al Zubaidi, N. Abbas, S. Nadeem Computational analysis of induced magnetohydrodynamic non-Newtonian nanofluid flow over nonlinear stretching sheet Prog React Kinet Mech, 47 (2) (2022).

13) Z. Abbas, M.Y. Rafiq Exploration of the dynamics of non-Newtonian Casson fluid subject to viscous dissipation and Joule heating between parallel walls due to buoyancy forces and pressure, Proc Inst Mech Eng Part E, 238 (2) (2023).

14) N. Ammar, H.A. Ali Mathematical modelling for peristaltic transport of non-Newtonian fluid through inclined non-uniform channel under the effect of surface roughness. Int J Nonlinear Anal Appl, 13 (2) (2022).

15) Farhan Ai, Zaib. A, Khalid. M Unsteady MHD Flow of casson fluid past Vertical Surface Using Laplace Transform Solution. Journal of Computational Biophysics and Chemistry, 2023, 22(3), 361-370.